

The band-gap structure and the singular character of the bounded large array of potential barriers

D. Bar^a

^aDepartment of Physics, Bar Ilan University, Ramat Gan, Israel.

Abstract

We have previously discussed the one dimensional multibarrier potential of finite range and found that under certain values of its total length L and the ratio c of total interval to total width it shows signs of chaos, phase transition and a transmission probability of unity. We show here that, like the infinite Kronig-Penney system which is arranged along the whole spatial region, the bounded multibarrier potential have a band-gap structure associated with its energy spectrum. But unlike the Kronig-Penney system in which the gaps disappear for large values of the energies here these gaps, because of their dependence upon L and c , do not disappear for certain values of these parameters. It will also be shown that the energy is discontinuous at many of its points even at the parts at which it has no gaps at all. We show that these results imply that the energy spectrum of the bounded multibarrier system is singular.

Pacs numbers; 71.15.Ap, 02.10.Yn, 03.65.Nk, 02.40.Xx

1 Introduction

It is known that the Kronig-Penney multibarrier system [1, 2] which is arranged along the whole spatial region is characterized by an energy spectrum that is composed of continuous bands separated by forbidden gaps [1, 2, 3]. The larger are the values of the energies the

shorter these gaps become until they entirely disappear for large enough energies [1, 2, 3]. It is also known [1] that the gaps in the energy spectrum of the infinite Kronig-Penney system are related [1] to the eigenvalues λ_{\pm} of the characteristic equation which is associated with the two dimensional transfer matrix that relates the transmission and reflection coefficients of any two neighbouring barriers. The limits $\lim_{n \rightarrow \pm\infty} \lambda_{\pm}^n$ are taken when the related potential barriers are separated from each other by a very large number n of other similar barriers. Thus, if either of these limits becomes very large, in which case the resulting wave function does not remain finite, then the corresponding energies are disallowed [1] and these constitute the gaps of the energy spectrum.

The former problems that are associated with the infinite Kronig-Penney system do not arise in the bounded multibarrier system discussed here. This is because although the number of barriers is very large, as for the Kronig-Penney system, nevertheless the finite extent of the system enables one to analytically express in explicit form [4, 5] the total transfer matrix that relates the two barriers at the two extreme sides of the system. Thus, the characteristic equation and the corresponding eigenvalues of this overall transfer matrix have also been found [5] in exact closed forms. From the latter one may construct the appropriate energy spectrum for both cases of $E > V$ and $E < V$ where E is the energy and V the constant height of all the barriers.

We show in the following that there are no allowed energies that correspond to certain values of the total length L of the system and the ratio c of its total interval to total width. Moreover, in contrast to the Kronig-Penney system in which the gaps in the energy spectrum disappear [1] for either large values of the energy E or (and) large values of the parameter (denoted κ here) over which E is plotted (see, for example Figure 6.6 in [1]) the case here is different. This is because, as will be shown in Sections 3-4, the gaps in the energy spectrum of the bounded one-dimensional multibarrier system do not disappear for certain values of L and c even for large E or (and) large κ . We also show that the energy E depends upon the total length L and the ratio c in such a manner that its form, as function of κ , is periodic

for small c and large (or intermediate) values of L and is proportional to κ for all $c > 3$. It will also be shown that the energy spectrum is discontinuous at many of its points even at the parts at which it has no gaps at all.

In Section 2 we introduce the terminology and terms [4, 5] that describe the bounded multibarrier potential. In Section 3 we discuss the energy spectrum for the $E > V$ case and find the values of the parameter κ for which no corresponding energies are found. That is, we find the band-gap structure of it. We also show the remarked discontinuity in E as function of κ . In Section 4 we repeat the whole process for the $E < V$ case and summarize in Table 1 the allowed energies for both cases of $E > V$ and $E < V$. In Section 5 we show that the occurrence of stable gaps in its energy spectrum together with other previously shown [4, 5] properties of it, imply that the bounded multibarrier potential is a singular system [6, 7, 8, 9, 10, 11]. We conclude with a brief summary in Section 6.

2 The bounded one-dimensional multibarrier potential

We consider a bounded one-dimensional system of N barriers assumed to have the same height V for all of them and to be uniformly arrayed between the point $x = -\frac{a+b}{2}$ and $x = \frac{a+b}{2}$. Thus, the total length of the system is $L = a + b$ where a denotes the total width of all the N barriers (where the potential $V \neq 0$), and b is the total sum of all the intervals between neighbouring barriers (where $V = 0$). That is, in a system of N barriers the width of each one is $\frac{a}{N}$, and the interval between each two neighbours is $\frac{b}{N-1}$. Writing b as $b = ac$, where c is a real number, we can express a and b in terms of L and c as [4]

$$a = \frac{L}{1+c}, \quad b = \frac{Lc}{1+c} \quad (1)$$

We consider the passage of a plane wave through this system, which has the form $\phi = A_0 e^{ikx} + B_0 e^{-ikx}$ where $x \leq -\frac{a+b}{2}$. Matching boundary conditions at the beginning and end

of each barrier, we may construct a solution in terms of the transfer matrix [1, 2, 12] $P^{(j)}$ on the j -th barrier. Thus, using the terminology in [1], we obtain after the n -th barrier the following transfer matrices equation [4]

$$\begin{bmatrix} A_{2n+1} \\ B_{2n+1} \end{bmatrix} = P^{(n)} P^{(n-1)} \dots P^{(2)} P^{(1)} \begin{bmatrix} A_0 \\ B_0 \end{bmatrix} = \mathcal{P} \begin{bmatrix} A_0 \\ B_0 \end{bmatrix}, \quad (2)$$

where A_{2n+1} and B_{2n+1} are the amplitudes of the transmitted and reflected parts [4, 5] respectively of the wave function at the n -th barrier. A_0 is the coefficient of the initial wave that approaches the potential barrier system, and B_0 is the coefficient of the reflected wave from the first barrier. \mathcal{P} is the total transfer matrix over the system of n barriers and is given for the $E > V$ case in the limit of large n by [4, 5]

$$\mathcal{P}_{E>V} = \begin{bmatrix} e^{-iz}(\cos \phi + if \frac{\sin(\phi)}{\phi}) & ie^{-iz}d \frac{\sin(\phi)}{\phi} \\ -e^{iz}d \frac{\sin(\phi)}{\phi} & e^{iz}(\cos \phi - if \frac{\sin(\phi)}{\phi}) \end{bmatrix} \quad (3)$$

The parameters f , d , z and ϕ are expressed as [4, 5]

$$f = kb + aq \frac{\xi}{2}, \quad d = aq \frac{\eta}{2}, \quad z = k(a + b), \quad \phi = \sqrt{f^2 - d^2}, \quad (4)$$

where k , q , ξ and η are [4, 5]

$$k = \sqrt{\frac{2m(E)}{\hbar^2}}, \quad q = \sqrt{\frac{2m(E - V)}{\hbar^2}}, \quad \xi = \frac{q}{k} + \frac{k}{q}, \quad \eta = \frac{q}{k} - \frac{k}{q} \quad (5)$$

It is shown [4, 5] that \mathcal{P} is given for the $E < V$ case and in the same limit of large n by

$$\mathcal{P}_{E<V} = \begin{bmatrix} e^{-iz}(\cos \phi + if \frac{\sin(\phi)}{\phi}) & -ie^{-iz}d \frac{\sin(\phi)}{\phi} \\ ie^{iz}d \frac{\sin(\phi)}{\phi} & e^{iz}(\cos \phi - if \frac{\sin(\phi)}{\phi}) \end{bmatrix}, \quad (6)$$

where the parameters \mathring{f} , \mathring{d} and $\mathring{\phi}$ are now

$$\mathring{f} = kb - \frac{aq\eta}{2}, \quad \mathring{d} = \frac{aq\xi}{2}, \quad \mathring{\phi} = \sqrt{\mathring{f}^2 - \mathring{d}^2}, \quad (7)$$

k is the same as for the $E > V$ case and $q = \sqrt{\frac{2m(V-E)}{\hbar^2}}$. In the numerical part of this work we follow the convention in the literature that assigns to \hbar and m the values of 1 and $\frac{1}{2}$ respectively. Defining, as in [5], the parameters κ and τ

$$e^{i\kappa} = \frac{\cos(\phi) + i\frac{f\sin(\phi)}{\phi}}{\sqrt{\cos^2(\phi) + \frac{f^2\sin^2(\phi)}{\phi^2}}}, \quad \tau = 1 + \frac{d^2\sin^2(\phi)}{\phi^2}, \quad (8)$$

one can obtain the eigenvalues of either the matrix of Eq (3) for the $E > V$ case or of the matrix (6) for $E < V$ in the form

$$\lambda_{1,2} = \tau \cos(\phi - \kappa) \pm \sqrt{\tau^2 \cos^2(\phi - \kappa) - 1} \quad (9)$$

The eigenvalues of the $E > V$ case are obtained by substituting the ϕ and f from Eq (4) and those of the $E < V$ case by substituting the corresponding quantities from Eq (7).

We, now, show that, unlike the infinite Kronig-Penney system [1, 2, 3] that have no finite total length L and no finite ratio c , the energy spectrum of the bounded multibarrier potential depends critically upon L and c . We first take the real components of both sides of the first of Eqs (8) and divide the numerator and denominator of its right hand side by $\cos(\phi)$

$$\cos(\kappa) = \frac{\cos(\phi)}{\sqrt{\cos^2(\phi) + \frac{f^2\sin^2(\phi)}{\phi^2}}} = \frac{1}{\sqrt{1 + \frac{f^2\tan^2(\phi)}{\phi^2}}} \quad (10)$$

We note that the last equation is valid for both cases of $E > V$ and $E < V$ except that one should substitute the appropriate f and ϕ from Eq (4) for the $E > V$ case as we do in next section or \mathring{f} and $\mathring{\phi}$ from Eq (7) for $E < V$ as done in Section 4.

3 The band-gap structure of the finite multibarrier system for the $E > V$ case

We, now, consider the $E > V$ case and substitute in Eq (10) the appropriate f , d , ϕ , k and q from Eqs (4)-(5) to obtain

$$\begin{aligned} \cos(\kappa) &= \frac{1}{\sqrt{1 + \left(1 + \frac{a^2 V^2}{4E(E(a+b)^2 - V(a^2 + ab))}\right) \tan^2(E(a+b)^2 - V(a^2 + ab))}} = \\ &= \frac{1}{\sqrt{1 + \left(1 + \frac{V^2}{4E(1+c)(E(1+c)-V)}\right) \tan^2(L^2(E - \frac{V}{1+c}))}} \end{aligned} \quad (11)$$

The last result was obtained by expressing a and b in terms of L and c according to Eq (1). Squaring both sides of the last equation one obtains

$$\cos^2(\kappa) = \frac{1}{1 + \left(1 + \frac{V^2}{4E(1+c)(E(1+c)-V)}\right) \tan^2(L^2(E - \frac{V}{1+c}))} \quad (12)$$

From Eq (12) we see that for all values of κ that cause $\cos^2(\kappa)$ on its left hand side to vanish one must have corresponding values of $L^2(E - \frac{V}{1+c})$ that cause $\tan^2(L^2(E - \frac{V}{1+c}))$ on its right hand side to become very large. That is, for $\kappa = \pm \frac{(2N+1)\pi}{2}$, ($N = 0, 1, 2, 3, \dots$) one must have $L^2(E - \frac{V}{1+c}) = \frac{(2N+1)\pi}{2}$, ($N = 0, 1, 2, 3, \dots$). Note that since E , V and c are positive the expression $L^2(E - \frac{V}{1+c})$ for the $E > V$ case is positive. Thus, the appropriate values of the energies E that correspond to the remarked values of κ are $E = \frac{(2N+1)\pi}{2L^2} + \frac{V}{1+c}$. That is, from the last expression for E and from the condition $E > V$ we find that there are allowed energies only for those values of the total length L and the ratio c that satisfy the inequality

$$\frac{(2N+1)(1+c)\pi}{2cL^2} > V, \quad N = 0, 1, 2, \dots \quad (13)$$

That is, the energies that correspond to $\kappa = \pm \frac{(2N+1)\pi}{2}$, ($N = 0, 1, 2, 3, \dots$) depend upon the total length L of the system and the ratio c of its total interval to total width. For all other

values of κ we may take the reciprocals of both sides of Eq (12) and subtract 1 from the resulting expressions to obtain

$$\tan^2(\kappa) = \left(1 + \frac{V^2}{4E(1+c)(E(1+c)-V)}\right) \tan^2\left(L^2\left(E - \frac{V}{1+c}\right)\right) \quad (14)$$

We note that exactly the same equations as those of (12) and (14) are obtained also for the $E < V$ case except that we use, as remarked, the \dot{f} and $\dot{\phi}$ from Eqs (7) with $q = \sqrt{\frac{2m(V-E)}{\hbar^2}}$ (where, for numerical purposes, we assign, as noted, $\hbar = 1$, and $m = \frac{1}{2}$). From Eq (14) we may find the energies that correspond to the values of κ that cause $\tan^2(\kappa)$ on its left hand side to vanish. These κ 's are $\kappa = \pm N\pi$, ($N = 0, 1, 2, 3 \dots$) so using Eq (14) and the positiveness of $L^2(E - \frac{V}{1+c})$ we have $L^2(E - \frac{V}{1+c}) = N\pi$ from which one obtains $E = \frac{N\pi}{L^2} + \frac{V}{1+c}$. From the last expression for E and from $E > V$ we find that there are allowed energies that correspond to $\kappa = \pm N\pi$, ($N = 0, 1, 2, 3 \dots$) only for those values of L and c that satisfy

$$\frac{N(1+c)\pi}{cL^2} > V, \quad N = 0, 1, 2, \dots \quad (15)$$

That is, as for the case of the inequality (13), the energies that correspond to $\kappa = \pm N\pi$, ($N = 0, 1, 2, 3 \dots$) depend upon the total length L of the system and the ratio c of its total interval to total width. Note that although $L^2(E - \frac{V}{1+c}) = 0$ corresponds also to the former values of κ that result in $\tan^2(\kappa) = 0$ there is no value of the energy E , for the $E > V$ case, that corresponds to $L^2(E - \frac{V}{1+c}) = 0$. This is because from $L^2(E - \frac{V}{1+c}) = 0$ one obtains $E = \frac{V}{1+c}$ which, for positive c , does not conform to $E > V$.

Now, as may be seen from Eq (14), the dependence of the allowed energies upon L , c and N is not restricted only to these values of E that correspond to $\kappa = \pm \frac{(2N+1)\pi}{2}$ or to $\kappa = \pm N\pi$, ($N = 0, 1, 2, 3 \dots$). Moreover, as will be shown in the following, the form of the allowed energy, as function of κ , depends in a peculiar manner upon the ratio c . That is, if c is small, say $0 < c < 3$, then the expression that multiply $\tan^2(L^2(E - \frac{V}{1+c}))$ on the right hand side of Eq (14) is larger than unity and the solution of Eq (14) for the allowed energy

E as function of κ can be obtained only numerically. In such case we find, as shown in the following, that these E 's change periodically with κ . If, on the other hand, $c \geq 3$ then the expression that multiply $\tan^2(L^2(E - \frac{V}{1+c}))$ on the right hand side of Eq (14) is very close to unity. For example, for $c = 3$ and $E \approx V$ this expression equals 1.020 and it tends fastly to unity for values of $c > 3$ or/and $E > V$. Thus, for $c > 3$ we may safely approximate Eq (14) as

$$\tan^2(\kappa) \approx \tan^2(L^2(E - \frac{V}{1+c})), \quad (16)$$

from which we obtain $\tan(L^2(E - \frac{V}{1+c})) = \pm \tan(\kappa)$. The last equation results in $L^2(E - \frac{V}{1+c}) = N\pi \pm \kappa$, ($N = 0, 1, 2, 3, \dots$) from which we have

$$E = \frac{N\pi \pm \kappa}{L^2} + \frac{V}{1+c}, \quad (N = 0, 1, 2, 3, \dots) \quad (17)$$

As seen from Eq (17) not all values of $N\pi \pm \kappa$ are suitable for the $E > V$ case but only those that satisfy $(N\pi \pm \kappa) > \frac{VL^2c}{1+c}$. For example, for $V = L = 15$ and $c = 3$ the permissible values of $N\pi \pm \kappa$ that have corresponding energies are only those that satisfy $(N\pi \pm \kappa) > 2531.25$.

For other values of c from the range $0 < c < 3$ the expression that multiplies $\tan^2(L^2(E - \frac{V}{1+c}))$ on the right hand side of Eq (14) is, as remarked, larger than unity for the $E > V$ case and one must resort to numerical methods for solving Eq (14) for E as function of κ . In this case the obtained energies are periodic where the spatial extent of the period and its amplitude depend upon the total length L of the system and the ratio c of its total interval to total width. It is also shown for both cases of $E > V$ and $E < V$ that the periodic character of the energy as function of κ emerges only for values of E that are close to the potential V (close from below for the $E < V$ case and from above for $E > V$). For example, for $V = 15$ the corresponding energy is found to periodically vary only between $E = 15.5$ and $E = 19.5$. This is because for higher values of E the expression that multiplies the *tangent* expression on the right hand side of Eq (14) tends to unity even for very small values of c . In such case the situation is the same as that formerly found for large c ($c > 3$) where the

appropriate equation to use is (16) which leads to the linear expressions (17) for the energy as function of κ . For values of E that are close to the potential V one may obtain not only the remarked periodic forms of the energy as function of κ but for very small c the allowed energies become constant as demonstrated by the horizontal lines in Figures 1-2. This is because for $E \approx v$ and $c \approx 0$ the right hand side of Eq (14) becomes the indeterminate form $\frac{0}{0}$, so using L'hospital theorem [15] we obtain for it the value of 1. In such case the value of $E \approx V$ does not change with κ .

The periodic nature of the energy as function of κ is demonstrated for small c in the form of half squares as seen from Figure 1 which shows nine different curves of E from Eq (14) as function of κ . All the nine curves are drawn for the same values of $V = 15$ and $L = 100$ but for 9 different values of the ratio $c = 0.2 \cdot n$, ($n = 1, 2, 3, \dots, 9$). The different graphs in this figure and in Figures 2-3 correspond to the values of c in a such a manner that the curves with the most pronounced periodic half squares, which are shown at the upper part of these figures, fit the lower values of c . The curves which are characterized by a short and flat periodic half squares, which are generally located at the lower parts of these figures, correspond to the higher values of c . The horizontal lines at the bottom of Figures 1 and 2 correspond, as remarked, to the constant value of the energy $E \approx V$. The remarked correspondence between the graphs of E and the appropriate c 's, by which the graphs at the upper part of the figure fit the lower c 's and those at the lower part of it fit the higher c 's, applies especially for the $E < V$ case in Figures 4-6.

As seen from Figure 1 any two neighbouring half squares are connected to each other by short horizontal lines where the energy is clearly discontinuous at the connecting points. That is, at these points the energy jumps in a discontinuous manner to form the squared parts where the smaller is c the larger are the corresponding jumps as may be seen at the higher part of the figure. For growing c the jumps become smaller and the corresponding half squares shorter as seen at the lower part of Figure 1. One may also realize that for the large value of L used in this figure the 9 different curves are shown mixed inside each other

between the two values of $E \approx 15.3$ and $E \approx 17.8$. Plotting the energies E as functions of κ for additional larger values of c , while keeping the same L as before, add more periodic forms (not shown) that are arrayed inside the formers between the same two limits of Figure 1.

We must note that taking into account the periodic character of the *tangent* function we can rewrite Eq (14) in its most general form as

$$\tan^2(\kappa \pm N\pi) = \left(1 + \frac{V^2}{4E(1+c)(E(1+c)-V)}\right) \tan^2\left(L^2\left(E - \frac{V}{1+c}\right) \pm \dot{N}\pi\right), \quad (18)$$

where $N, \dot{N} = 0, 1, 2, \dots$. Since the parameter L occurs only under the *tangent* function at the right hand side of the last equation we may numerically solve it for E and find the same periodic dependence upon κ for different values of L . For example, Figure 4, which was drawn for $L = 30$ may be obtained in almost the same form for $L = 110$. Figures 1-6 of this work are obtained from the equivalent equation (14) in which $\dot{N}, N = 0$. Note that for very small L one may approximate the *tangent* function at the right hand side of Eq (14) by $L^2\left(E - \frac{V}{1+c}\right)$ and numerically solves the resulting equation for E as function of κ . The resulting spectrum is shown in Figure 3 for the $E > V$ case and in Figures 6-7 for $E < V$.

As L decreases in value the different curves begin to be separated from each other and to occupy different sections of the ordinate axis. This is shown in Figures 2 and 3 which are drawn under exactly the same conditions and for the same values of V and c as in Figure 1 except that now L assumes the values of $L = 5$ for the curves of Figure 2 and $L = 0.3$ for those of Figure 3. The highest periodic half squares of Figure 2 are drawn around the value of $E = 19.6$ and those of Figure 3 around $E = 29$. Note that the half squares of Figure 2 are each connected to the horizontal linear sections at more than two points (compare with Figure 1). This is especially demonstrated in the curves at the higher part of Figure 2 which correspond to the smaller values of c . Also, as in Figure 1 the discontinuous jumps in the energy are larger for the curves that correspond to small c 's at the upper part of Figure 2

and smaller for the larger c 's at the lower part of it. The periodic curves of Figure 3 which are all drawn for the value of $L = 0.3$ are seen to be rather curved than squared and the points at which the energy jumps to form the pronounced parts of it are two for each period as in Figure 1. Also, the larger is the value of c at the lower part of Figure 3 the smaller become the corresponding jumps of E .

4 The band-gap structure of the finite multibarrier system for the $E < V$ case

We, now, discuss the $E < V$ case and begin from Eq (12) which is valid, as remarked, also for this case. We find first the allowed energies that correspond to the values of κ that cause the left hand side of Eq (12) to vanish, that is, to $\kappa = \pm \frac{(2N+1)\pi}{2}$, ($N = 0, 1, 2, 3, \dots$). As for the $E > V$ case these energies are $E = \pm \frac{(2N+1)\pi}{2L^2} + \frac{V}{1+c}$ but now we consider also the E 's that correspond to negative values of κ so long as this does not cause the energies to become negative. That is, considering the negative values of κ we obtain from the last inline equation for E and from $E > 0$ that L , c and V should be related by the inequality $\frac{(2N+1)\pi}{2L^2} < \frac{V}{1+c}$ in which case L could not be very small. Thus, taking into account both positive and negative values of κ and the condition $E < V$ we see that there exist allowed energies only for those values of L and c that satisfy

$$\pm \frac{(2N+1)(1+c)\pi}{2cL^2} < V, \quad (N = 0, 1, 2, \dots) \quad (19)$$

In order to satisfy the last inequality for the case in which the minus sign at the left hand side is considered the parameters L , c and V must also be related, as remarked, by $\frac{(2N+1)\pi}{2L^2} < \frac{V}{1+c}$. Comparing Inequality (19) with that of (13) we see that, as for the $E > V$ case, the allowed energies that correspond to $\kappa = \pm \frac{(2N+1)\pi}{2}$, ($N = 0, 1, 2, 3, \dots$) depend critically upon the values of the total length L and the ratio c . Note that whereas in the $E > V$ case there are

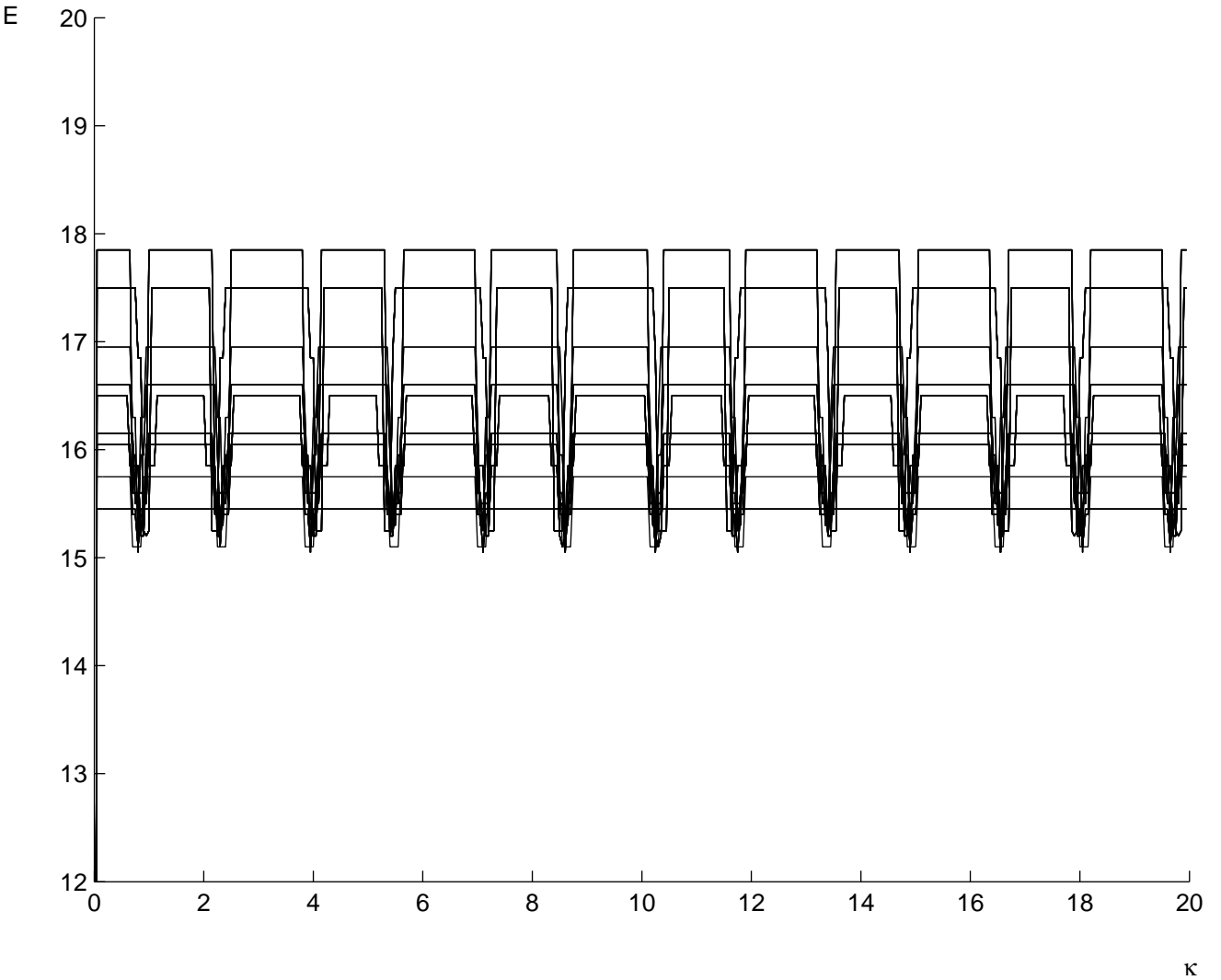


Figure 1: The nine graphs of this figure, which show the energy E from Eq (14) as function of κ , are all drawn for the same values of $V = 15$ and $L = 100$ and for nine different values of the ratio $c = 0.2 \cdot n$, ($n = 1, 2, \dots, 9$). The curves that have pronounced half squares at the higher part of the figure fit the lower values of c and those that have short and flat squared parts belong to the higher c 's. The horizontal line at the bottom corresponds to the constant value of the energy obtained at $E \approx V$. Each periodic half square is connected at its two sides by short horizontal linear sections. One may clearly see that the energy is discontinuous and undifferentiable at the vertical sides of each half square.

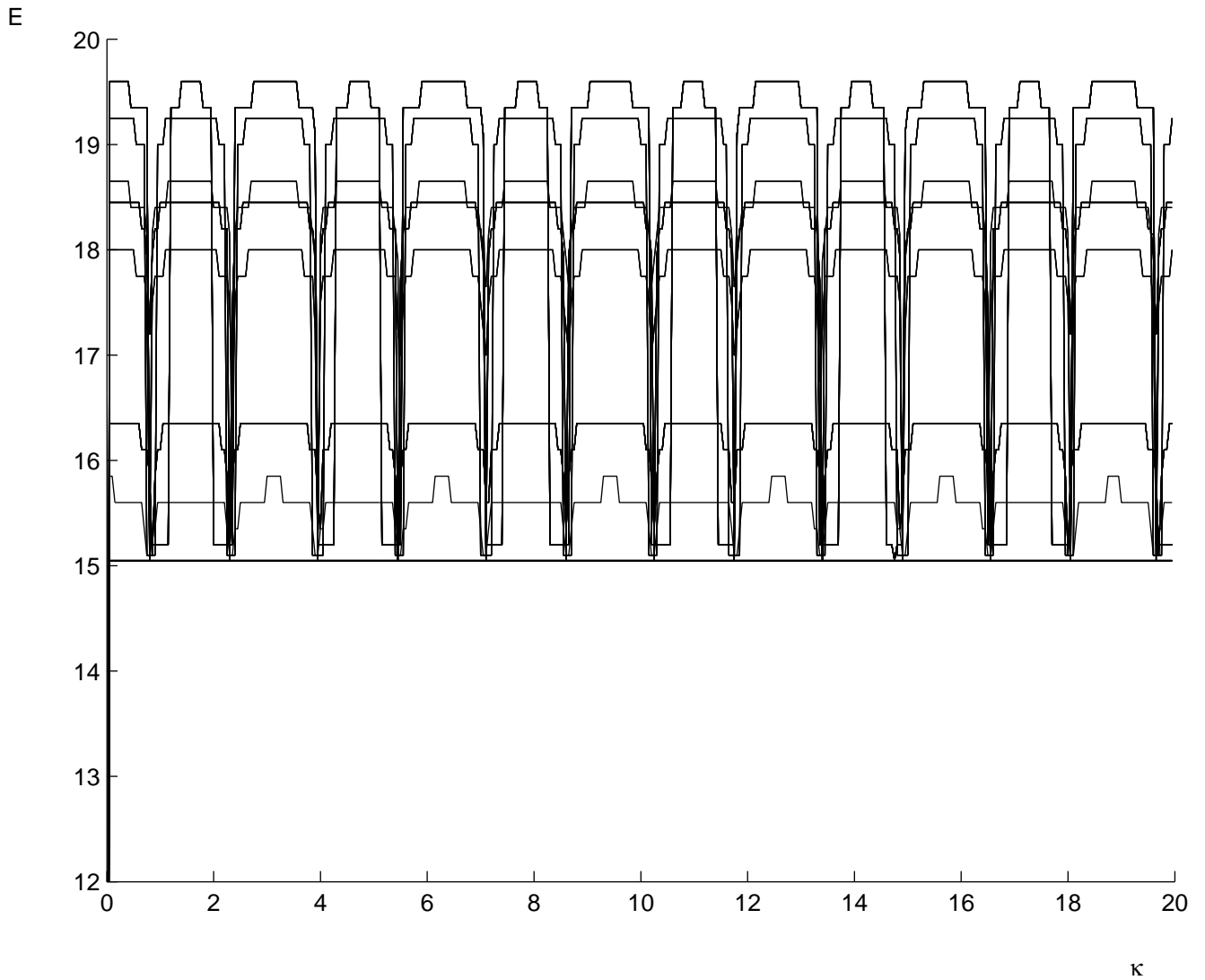


Figure 2: The nine graphs in this figure, which show the energy E from Eq (14) as function of κ , are drawn under exactly the same conditions as those of Figure 1 except that now $L = 5$. One may see that the graphs are now separated from each other, especially those at the higher part of the figure which are clearly detached from the lower three graphs. Note that each half square, especially at the higher part of the figure, is discontinuous at several points and not at only its two sides (compare with Figure 1). The horizontal line at the bottom corresponds to the constant value $E \approx V$.

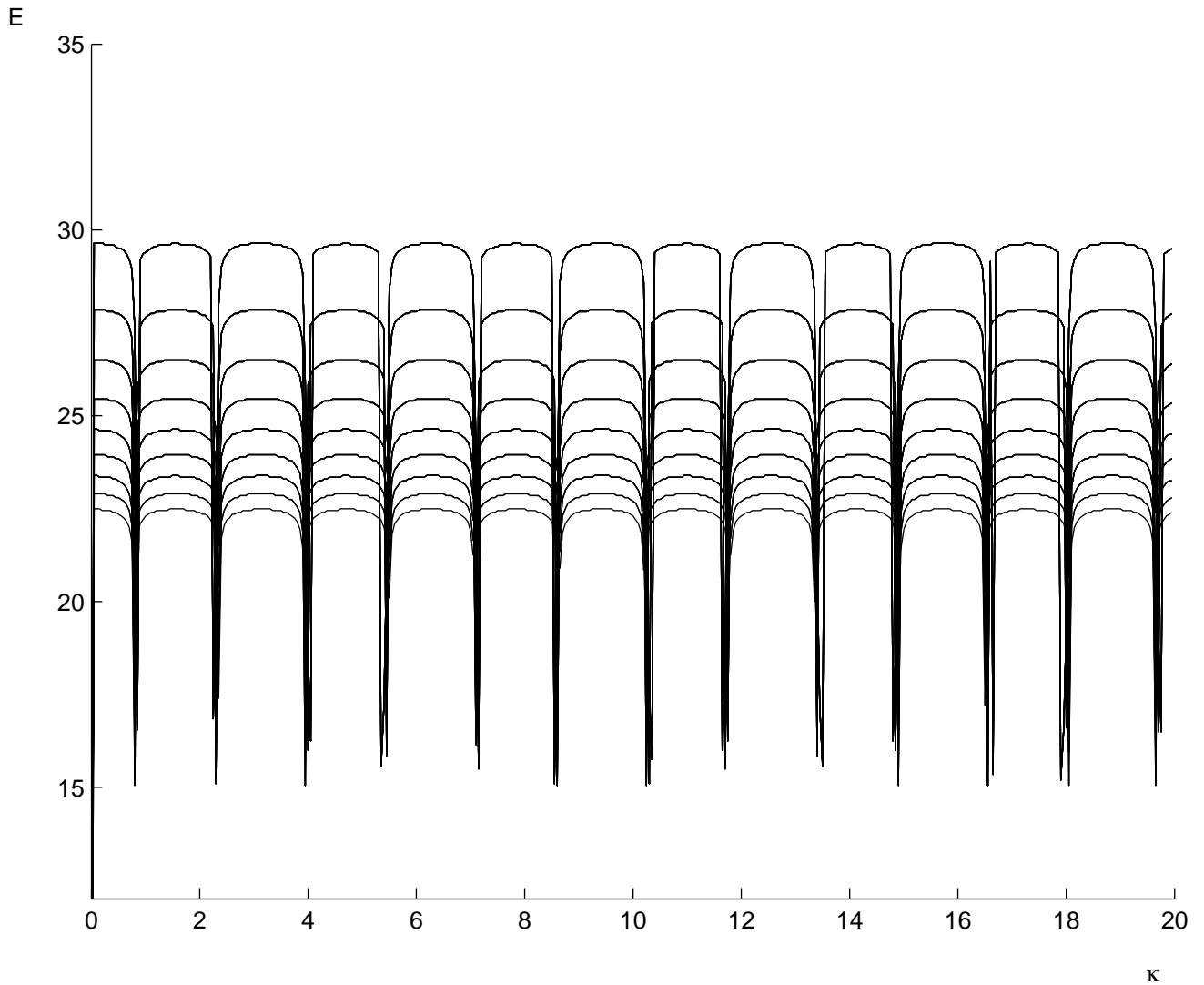


Figure 3: In this figure, which is composed as in Figures 1-2 of nine graphs of the energy E as function of κ , the total length L is further decreased for all the graphs to $L = 0.3$. The values of V and c remain as in Figures 1-2. Note that this additional decrease of L causes the periodic half squares to be narrower, more curved and arranged separately from each other compared to Figures 1-2.

no allowed energies for the very large values of either L or c (or both, see Inequality (13)), here, when considering the plus sign at the left hand side of (19), we find no such allowed energies for the very small values of either L or c (or both).

We, now, find the allowed energies that correspond to the values of κ that cause the left hand side of Eq (14) to vanish, that is, to $\kappa = \pm N\pi$, ($N = 0, 1, 2, 3 \dots$). These energies are found, as for the $E > V$ case, from $L^2(E - \frac{V}{1+c}) = \pm N\pi$ and are $E = \pm \frac{N\pi}{L^2} + \frac{V}{1+c}$. Using the former discussion at the beginning of this section we conclude that we may consider also negative κ 's so long as $\frac{N\pi}{L^2} < \frac{V}{1+c}$ in which case L could not be very small. Thus, considering both positive and negative values of κ and the $E < V$ condition we find that there are allowed energies that correspond to $\kappa = \pm N\pi$, ($N = 0, 1, 2, 3 \dots$) only for L and c that satisfy

$$\pm \frac{N(1+c)\pi}{cL^2} < V, \quad (N = 0, 1, 2, \dots) \quad (20)$$

In order to satisfy the last inequality for the case in which the minus sign at its left hand side is considered the parameters L , c and V must be related also by $\frac{N\pi}{L^2} < \frac{V}{1+c}$. Comparing Inequality (20) with that of (15), which refers to the $E > V$ case, we find a result analogous to that formerly found from comparing the Inequalities (13) and (19). That is, considering the plus sign at the left hand side of (20), one may realize that for very small values of either L or c or both of them there are no allowed energies that correspond to $\kappa = \pm N\pi$, ($N = 0, 1, 2, \dots$). This is to be compared to the corresponding $E > V$ case and the Inequality (15) from which one finds that there are no allowed energies for the very large values of either L or c or both of them.

As realized from Eq (14), which is valid also for the $E < V$ case, the dependence of the allowed energies upon L and c is not restricted only to these values that correspond to $\kappa = \pm \frac{(2N+1)\pi}{2}$ or to $\kappa = \pm N\pi$, ($N = 0, 1, 2, 3 \dots$). Thus, one may find also the energies that correspond to other values of κ but in this case we have first to exclude those values of E that cause the expression that multiply $\tan^2(L^2(E - \frac{V}{1+c}))$ on the right hand side of Eq (14)

to become negative. Otherwise, the right hand side of Eq (14) would be negative whereas its left hand side is positive. Thus, the allowed energies are those that satisfy

$$\frac{V^2}{4E(1+c)(E(1+c)-V)} > -1 \quad (21)$$

The last inequality results in

$$E^2 - E \frac{V}{1+c} + \frac{V^2}{4(1+c)^2} > 0, \quad (22)$$

from which one may conclude that the allowed energies of the bounded multibarrier system for the $E < V$ case should be only those that satisfy the inequality

$$v > E > \frac{V}{1+c} \quad (23)$$

Thus, the energies that correspond to $\kappa \neq \pm \frac{(2N+1)\pi}{2}$ and $\kappa \neq \pm N\pi$ should belong to the range $V > E > \frac{V}{1+c}$ which means that for very small values of c there are no allowed values of E at all. For not very small c the energies are found by discussing, as in the $E > V$ case, the two cases of large and small c . That is, for values of E that are close to V (but always $E < V$) the expression that multiplies $\tan^2(L^2(E - \frac{V}{1+c}))$ on the right hand side of Eq (14) tends to unity for $c > 3$. In such case we may use, as in the $E > V$ case, the simpler Eq (16) that results with the expression (17) for the allowed energies. But now since, as remarked, E satisfies $V > E > \frac{V}{1+c}$ there are corresponding energies only for $0 < N\pi \pm \kappa < \frac{vL^2c}{1+c}$, ($N = 0, 1, 2, \dots$). Thus, using Eq (17), which is valid also for the $E < V$ case, we find that the energies that correspond to $c > 3$ and that are close from below to V are allowed only for κ , c , L and V that are related by

$$\frac{(1+c)(N\pi \pm \kappa)}{L^2c} < V \quad (24)$$

For values of c from the range $0 < c < 3$ and for energies that are not close to V we use the full equation (14) which necessitates numerical methods for solving it for E as function of κ . It is found, as in the $E > V$ case, that the required energies are either periodic or constant. The constant energies are demonstrated by horizontal lines and appear when E assumes the value of $E \approx \frac{V}{1+c}$. In this case the right hand side of Eq (14) assumes the indeterminate form $\frac{0}{0}$ so using L'hospital theorem [15] it becomes unity for all values of κ . The analogous cases discussed in the former section for $E > V$ resulted in finding constant horizontal lines for $E \approx v$. Each of the following three Figures 4-6 shows 14 different graphs of the energy E as function of κ for the same value of $v = 15$ and for $c = 0.2 \cdot n$, $n = 1, 2, 3, \dots, 14$. As for Figures 1-3 the 14 curves in each figure of the set 4-6 fit the 14 values of c in an inverted order. That is, the highest value of c fits the lowest curve in each figure and the second value of c from above corresponds to the second curve from below in each figure and so forth. The 14 graphs of Figure 4 are all drawn for the value of $L = 30$ and one may see how the energy, in the form of half squares, changes periodically with κ . One may also realize that the most pronounced half squares are obtained for the smallest value assumed here for c ($c = 0.2$). Each half square is connected at its two sides to its neighbours by horizontal lines where, as for the $E > V$ case, the energy jumps at the connecting points in a discontinuous manner. Note that the larger is c at the lower part of the figure the longer become the connecting horizontal lines between the half squares which become shorter and narrower. The 14 different graphs of the energy E as function of κ , which are shown in Figure 5, are all drawn for the same values of V and c as those of Figure 4 but for $L = 5$. The periodic squared sections are now less emphasized compared to those of Figure 4 and they become flattened for the larger values of c as seen in the curves at the lower part of the figure. Also, compared to Figure 4, each squared section is connected, especially at the higher part of Figure 5, to more than two points at which the energy jumps discontinuously. From Figures 4-5 and from the occurrence of L^2 under the *tangent* function in Eq (14) one may realize that decreasing the value of L results in a corresponding decrease of the height

and width of the periodic squared sections. This is clearly shown in Figure 6 which shows 14 graphs of E as function of κ that are drawn under exactly the same conditions and the same values of V and c as those of Figures 4-5 except that now L assumes the rather small value of $L = 0.8$. The periodic parts, that are no longer half squares, have been considerably flattened to the degree of becoming almost horizontal lines as seen clearly in the curves at the lower part of the figure.

Continuing to further decrease the parameter L results in widening the gaps in the energy spectrum, that is, in finding no corresponding allowed energies for larger ranges of the κ axis. This is clearly shown in Figure 7 which shows the form of E as function of κ for the same $V = 15$ and $c = 0.2 \cdot n$, $n = 1, 2, 3, \dots, 14$ as those of Figures 1-6 but for $L = 0.278$. As seen from the figure the allowed energies are represented by the separate vertical lines between $E = 5$ and $E = 15$. Note that each vertical line is actually composed of 14 short vertical sections that correspond to the 14 different values of $c = 0.2 \cdot n$, $n = 1, 2, 3, \dots, 14$. That is, for this small value of L the energies for the different c 's are very similar to each other. As seen, the gaps between the allowed energies are periodically repeated over the positive side of the κ axis and do not vanish for any value of it. This result denotes, as will be shown in the next section, that the bounded multibarrier potential is singular for this value of L .

In Table 1 we show the allowed energy E and its dependence upon κ , L , c and V for both cases of $E > V$ and $E < V$.

5 The singular character of the bounded multibarrier system

We have seen in the former Sections 3-4 that the bounded multibarrier potential have gaps associated with its energy spectrum which depend upon the total length L of the system and the ratio c of its total interval to total width. We also show that, unlike the gap-band structure of the infinite Kronig-Penney system [1] in which the gaps disappear for large

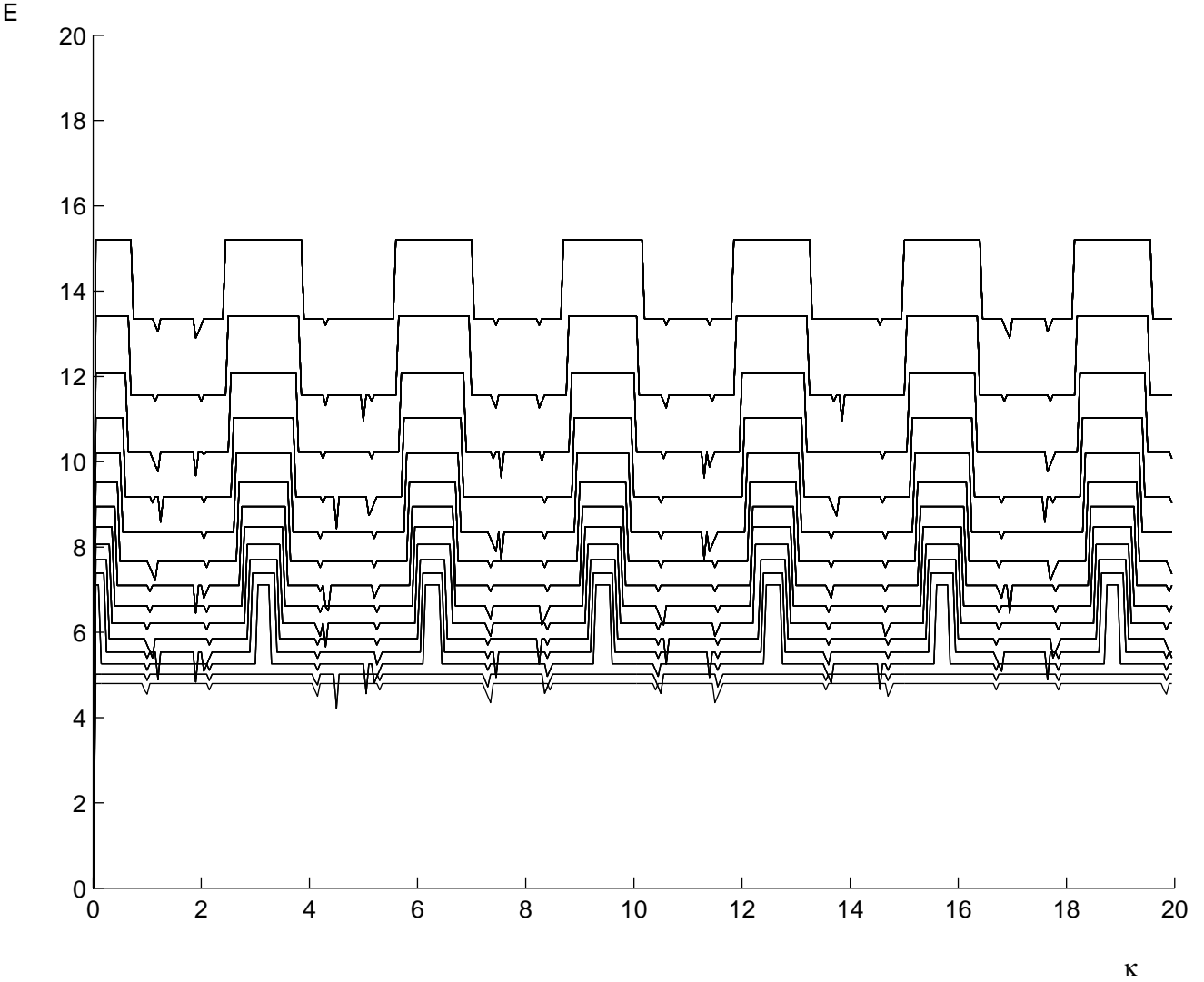


Figure 4: The 14 graphs of this figure show the energy E from Eq (14) as function of κ for the same $V = 15$ and $L = 30$ but 14 different values of $c = 0.2 \cdot n$, ($n = 1, 2, \dots, 14$). The allowed energies are found in the range $\frac{V}{1+c} < E < V$. The graphs fit the values of c in an inverted order, that is, the higher c 's correspond to the lower curves of the figure and vice versa. Note that for this value of $L = 30$ the periodic half squares are large and separated for the smaller c 's at the higher part of the figure while they become narrow and flat for the larger c 's at the lower part of it.

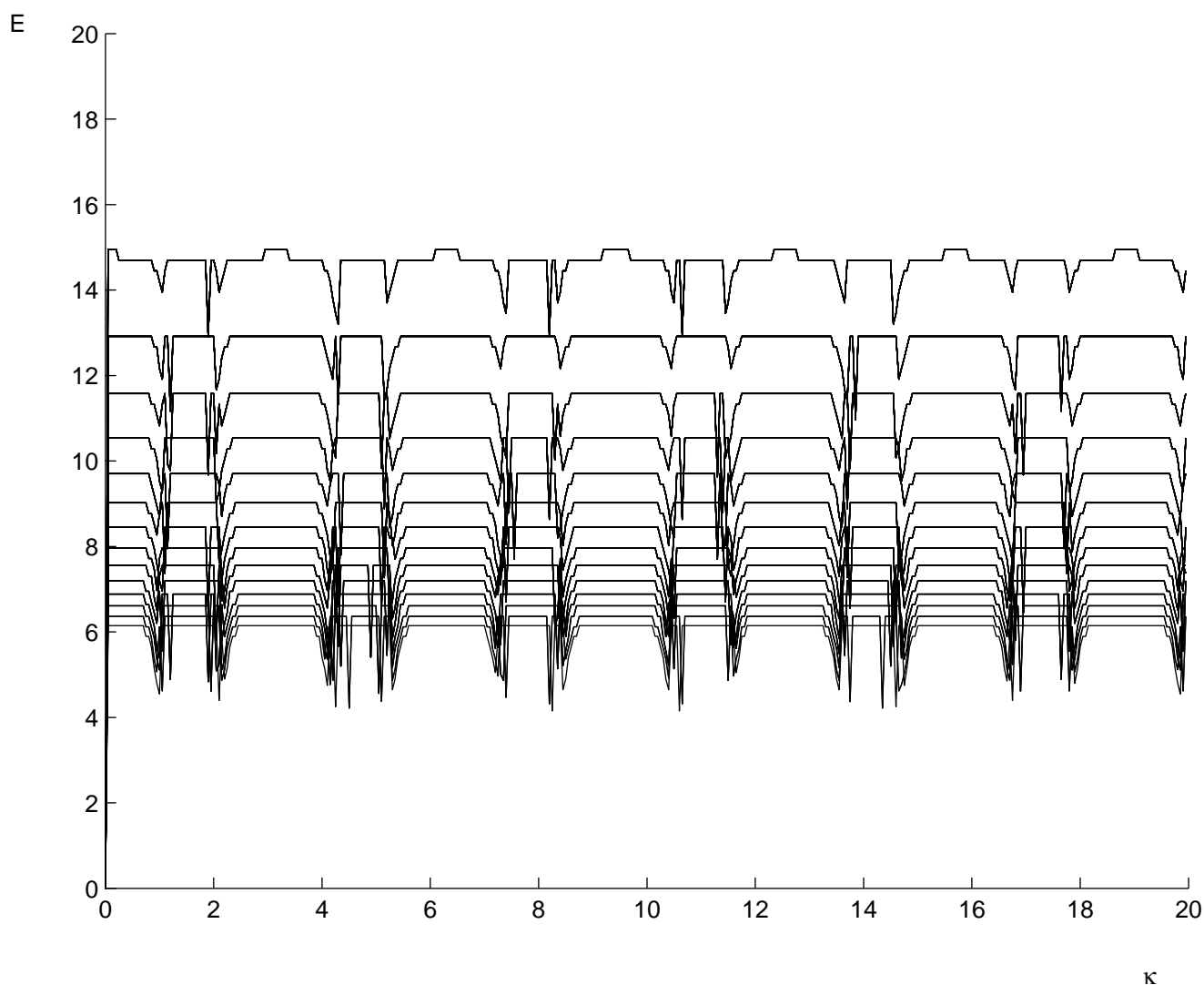


Figure 5: All the 14 graphs of this figure, which show the energy E from Eq (14) as function of κ , are drawn for the same $V = 15$ and the same range of $c = 0.2 \cdot n$, ($n = 1, 2, \dots, 14$) as those of Figure 4 but for the lower value of $L = 5$. As for Figure 4 the curves fit the values of c in descending order so that the lower values of c correspond to the curves at the higher part of the figure and the higher c 's fit the curves at the lower part of it. Note that the periodic squared sections are less pronounced than those of Figure 4 and they become almost horizontal lines for the higher c 's at the lower graphs.

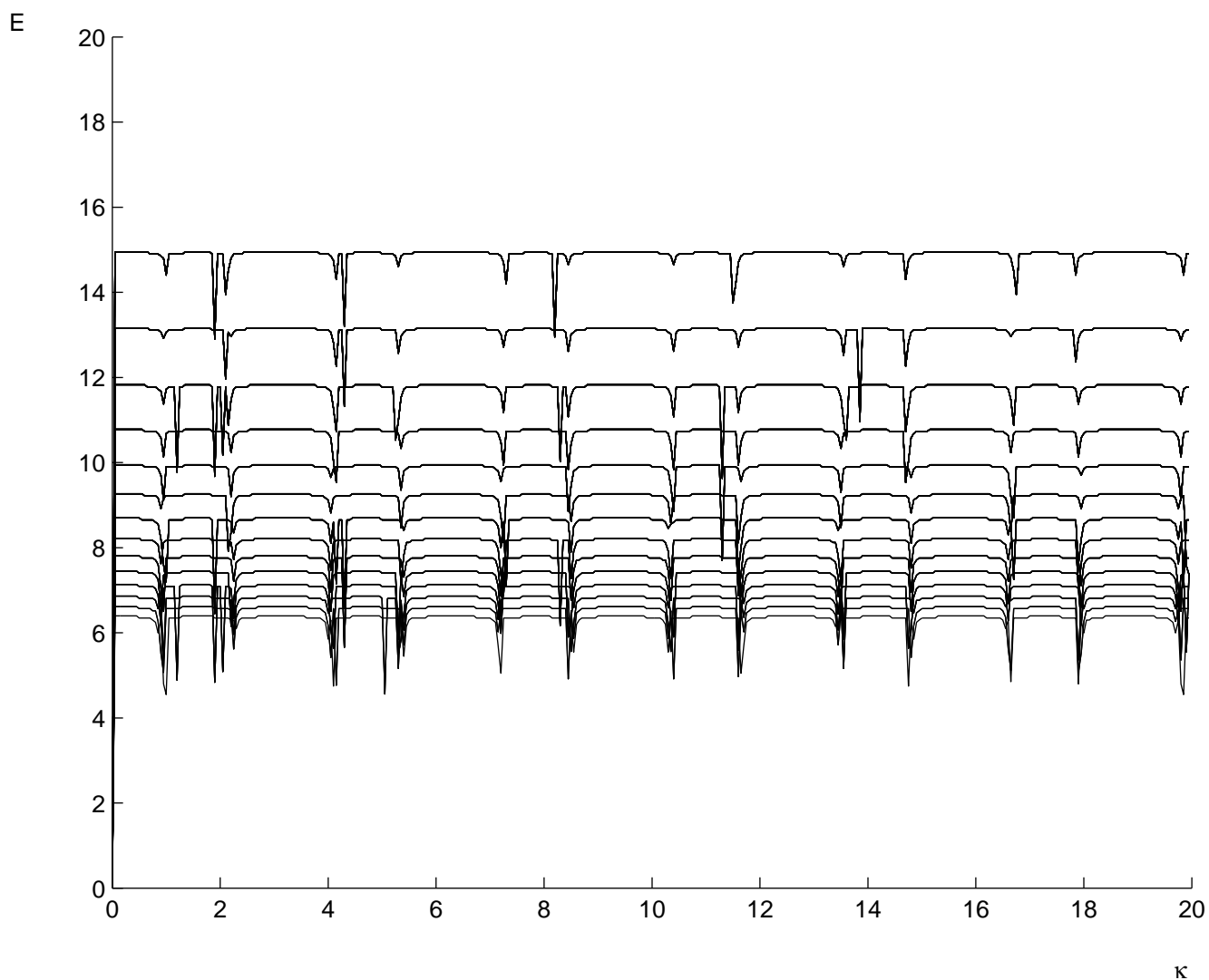


Figure 6: The 14 graphs of this figure, which show the energy E as function of κ , are drawn under exactly the same conditions and the same V and range of c as those of Figures 4-5 except that now L is decreased to the value of $L = 0.8$. Note that the curves become almost horizontal lines and this is further emphasized for the higher values of c in the lower graphs of the figure. Also, one may see that the discontinuity encountered for the larger values of L in Figures 4-5 is now less pronounced.

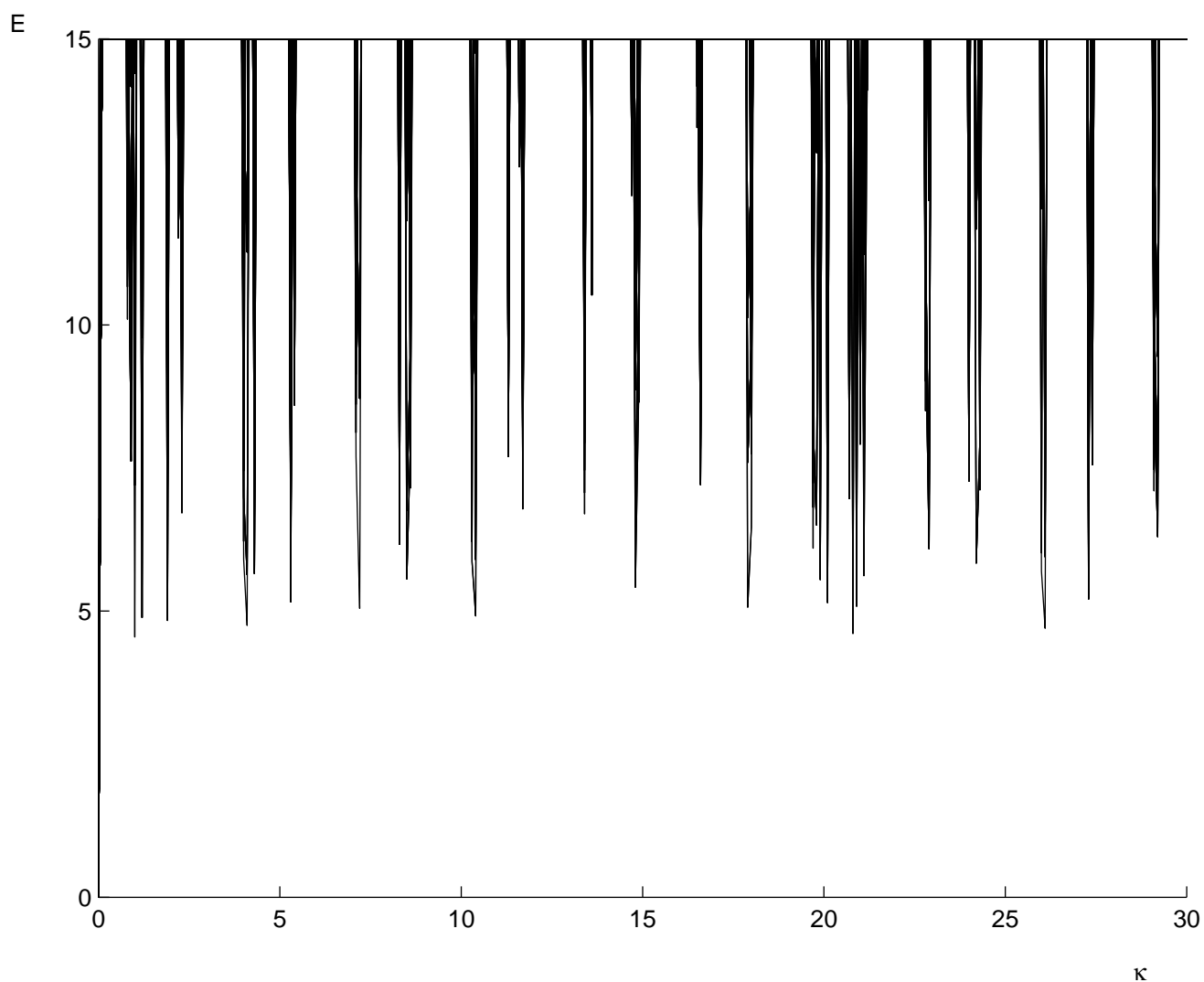


Figure 7: This figure shows the form of the energy E , for the $E < V$ case as function of κ , for the same $V = 15$ and the same values of $c = 0.2 \cdot n$, $n = 1, 2, 3, \dots, 14$ as those of Figures 4-6 except that now L is further decreased to the value of $L = 0.278$. As seen, the allowed energies are represented by the separate vertical lines between $E = 5$ and $E = 15$ where each line is composed of 14 short sections of E that correspond to the 14 different c 's. One may realize that the gaps for this small L are periodically repeated over the whole positive κ axis and do not vanish for any value of it.

Table 1: The table shows the allowed energy E for specific values of κ and for both cases of $E > V$ and $E < V$. We may realize from the table that the allowed energies of the bounded multibarrier potential depend critically upon the total length L and the ratio c . Thus, one may conclude that for certain values of L and c there are no corresponding energies as discussed in details in Sections 3 and 4. Also, there are no energies, especially, in the limits of very small L or c (or both) for the $E < V$ case and in the limits of very large L or c (or both) for the $E > V$ case. By N we mean all the natural numbers and zero ($N = 0, 1, 2, 3, \dots$).

κ, c	$E > V$	$E < V$
For all κ and small c $\kappa = \frac{(2N+1)\pi}{2}$ $\kappa = -\frac{(2N+1)\pi}{2}$ $\kappa = N\pi$ $\kappa = -N\pi$ $N\pi \pm \kappa, \kappa \neq \pm N\pi, \kappa \neq \pm \frac{(2N+1)\pi}{2}, c > 3,$ $N\pi \pm \kappa, \kappa \neq \pm N\pi, \kappa \neq \pm \frac{(2N+1)\pi}{2}, 0 < c < 3,$	E constant for $E \approx v$ $E = \frac{(2N+1)\pi}{2L^2} + \frac{V}{1+c}$ $E = \frac{(2N+1)\pi}{2L^2} + \frac{V}{1+c}$ $e = \frac{N\pi}{L^2} + \frac{V}{1+c}$ $e = \frac{N\pi}{L^2} + \frac{V}{1+c}$ $E = \frac{N\pi \pm \kappa}{L^2} + \frac{V}{1+c}$ (periodic, see text)	E constant for $E \approx \frac{V}{1+c}$ $E = \frac{(2N+1)\pi}{2L^2} + \frac{V}{1+c}$ $E = -\frac{(2N+1)\pi}{2L^2} + \frac{V}{1+c}$ $E = \frac{N\pi}{L^2} + \frac{V}{1+c}$ $E = -\frac{N\pi}{L^2} + \frac{V}{1+c}$ $\frac{V}{1+c} < E = \frac{N\pi \pm \kappa}{L^2} + \frac{V}{1+c} < V$ (periodic, see text)

values of the energy, here the remarked dependence of the energy spectrum upon L and c implied that for certain values of them the gaps do not disappear in any case. This has been shown for the $E > V$ case in Section 3 and especially for $E < V$ in Section 4 where we see that there are no energies that satisfy $E \leq \frac{V}{(1+c)}$ (see Inequality (23)). Now, it is accepted in the literature (see, for example, [7, 8]) that if the energy spectrum of any system have gaps that do not diminish for either large values of the energy E or large κ then the relevant system is considered singular. We show in Sections 3-4 that the energy spectrum of the bounded multibarrier potential not only have gaps that remain constant for all values of κ but that even for the parts of the epectrum that have no gaps there are points at which the energy, as function of κ , is discontinuous. These points are shown, for both cases of $E > V$ and $E < V$, to be associated with large L and small c as seen in the higher parts of Figures 1-2 and 4-5. Only at small L one may obtain energies that change continuously with κ and do not jump in a discontinuous manner (see Figures 3 and 6). Thus, the existence of the points at which the energy changes discontinuously with κ together with the remarked nonvanishing gaps demonstrate that the bounded multibarrier potential is singular. This

may be corroborated by a result obtained previously [4] which shows that the transmission probability of the bounded one-dimensional multibarrier is unity. That is, the incoming wave function remains the same (preserved) after passing the dense array of potential barriers [4]. The three properties of; (1) zero range potential, (2) nonvanishing gaps and (3) the ability to pass all the barriers of the system are characterized in the literature [6, 7, 8, 9] as signs of singular systems. All the former three properties characterize also the bounded multibarrier potential discussed here so this system must be singular. A singular behaviour of the energy spectrum is demonstrated also in what is termed the singular point interaction δ that is characterized by a periodic array of identical short-range perturbations [6, 8, 9] like our system. The allowed bands resulting from this δ interaction are characterized [8] by an increasing, as E grows, of the gap to band ratio. The only difference between the periodic singular interaction δ and our system is that the former is infinite [8], whereas our system is bounded.

We note that the infiniteness of the physical system is also what characterizes many examples discussed in [7], so the physical interpretation of the singular continuity of these systems (see [7, 8]) is connected to their infinity. That is, as written in [7] *the particle will be transmitted at least once through each barrier and then it will return again to the initial point from which it has started*. Thus, for these infinite systems the singular continuity is characterized by complete reflection that follows a former stage during which all the barriers are transmitted. This is so for the infinite systems in which no kind of transmission is possible at all, but since the bounded system admits transmission then the particle after passing all barriers found itself outside the system at the other side of it and not at its initial side. Thus, what characterizes its singular continuity is *complete transmission after the particle has been transmitted through each barrier*. This was clearly shown [4], using transfer matrix methods [1, 2, 12], for the bounded system discussed here. We, now, show this again by using the same analytical methods applied in [8] for showing complete reflection of the δ system. That is, taking into account the properties of the bounded multibarrier system and

incorporating them into the formalism of [8] we show that one obtains complete transmission instead of complete reflection. The single change we introduce into the formalism in [8] is that of bounding the length of the system so that, as we show, complete transmission is obtained instead of the total reflection of the unbounded system. In [8] the multi-channels [9] version of the δ interaction is discussed so that all possible kinds of interactions are taken into account (elastic, inelastic etc). The physical system used in [8] is an infinite sequence of onionlike N channels scatterers, so that the reflection amplitude from any such scatterer is given in [8] by

$$R = \frac{-N^2 + 1}{N^2 + 2iN \cot(kl) + 1}, \quad (25)$$

where l is the length of each scatterer [8] and $k = \sqrt{\frac{2mc}{\hbar^2}}$. The total reflection character of this system is demonstrated [8] when the length l tends to zero and the number N of channels in each scatterer becomes very much large. In these limits one may write [8] $\cot(kl) \approx \frac{1}{kl}$ and the unity term in Eq (25) may be discarded compared to N^2 . Thus, denoting, as in [8], the product Nl by β the reflection amplitude from equation (25) becomes [8]

$$R = -(1 + \frac{2i}{\beta k})^{-1} \quad (26)$$

When, as in [8], $k \rightarrow \infty$ (and still $kl \ll 1$), the product βk satisfies, due to the large N , $\beta k = kNl \rightarrow \infty$ and the reflection amplitude tends to -1 so that the reflection probability R^2 becomes $R^2 \rightarrow 1$. Now, we show that if the system is finite the reflection is zero in two cases: when either the number of channels N is large, or when $N = 1$ as in the dense array of potential barriers for which there exists only one kind of interaction. The length of each scatterer (barrier) is now $l = \frac{L}{n}$ where L , for the bounded system, signifies the total length of all the scatterers (barriers), and is some finite number. N is the number of channels in each scatterer and n is the number of scatterers in the bounded system, where obviously $n \gg N$. We begin from the case of large N and take into account that the number of barriers n in the bounded system, for either large or small N , is always very large, actually $n \rightarrow \infty$. Thus,

denoting as before the product of the length of each scatterer and N by β (so as to have now $lN = \frac{LN}{n} = \beta$) and using the former approximations of $\cot(kl) \approx \frac{1}{kl}$ and $N^2 + 1 \approx N^2$, we may write Eq (25) as

$$\begin{aligned} R &= \frac{-N^2 + 1}{N^2 + 2iN \cot(\frac{kL}{n}) + 1} = \frac{-N^2 + 1}{N^2 + \frac{2iN^2}{k\beta} + 1} \approx \\ &\approx \frac{-N^2}{N^2(1 + \frac{2i}{k\beta})} = -(1 + \frac{2i}{k\beta})^{-1} \end{aligned} \quad (27)$$

Now, when $k \rightarrow \infty$ (and still $kl = \frac{kL}{n} \ll 1$ as for the analogous case of Eq (26)) we have now, due to $n \gg N$, $k\beta = \frac{kLN}{n} \ll 1$, and the reflection amplitude goes to zero in contrast to the result obtained from Eq (26). Thus, from the relation between the reflection and transmission amplitudes $T = 1 - R$, we learn that T goes to 1 as required. That is, we see that if the length of the sequence of scatterers is finite and if it is dense enough so that the number of scatterers n is very large then the transmission coefficient goes to 1 for large number of channels N in each scatterer. The same result is trivially obtained for the case of a single channel for each scatterer, that is, $N = 1$ which is the case dealt with here. That is, substituting $N = 1$ in either Eq (25) or Eq (27) we obtain $R = 0$ so that $T = 1$.

Thus, we see, as remarked, that the singular character of the bounded dense array of potential barriers is affected through the complete transmission it demonstrates.

6 Concluding Remarks

We have found the allowed energies of the bounded one-dimensional multibarrier potential for both cases of $E > V$ and $E < V$. These allowed energies critically depend upon the values of the total length L of the system and the ratio c of its total interval to total width. Thus, it has been shown that there are values of L and c for which there are no allowed energies. For example, it has been demonstrated in Section 4 for the $E < V$ case that the allowed energies are only those from the range $V > E > \frac{V}{1+c}$. That is, for very small values of c there exist

no energy for the bounded multibarrier system.

It has, also, been shown for both cases of $E > V$ and $E < V$ that for small c and large (or intermediate) values of L the energy E have the form of periodic half squares which are connected to each other by horizontal lines. The points of connection of these half squares, as may be seen from the figures, are points of discontinuity at which the energy can not be differentiated. For small values of L these squared parts become shorter, narrower and more curved (see Figures 3 and 6) until they disappear for small enough L in which case the energy, as function of κ , resembles the form of either horizontal (or vertical lines for the $E < V$ case, see Figure 7).

The remarked existence of gaps that do not disappear for certain values of L and c , even for large κ 's, implied that the spectrum of the bounded multibarrier potential is singular. For example, it has been found for the $E < V$ case and for very small L that the allowed energies have the form of short vertical lines that have wide gaps between them as seen in Figure 7. These gaps are periodic and do not vanish for any value of κ . The constancy of the gaps in the energy spectrum of other physical systems, like the δ mentioned in Section 5, is interpreted in the literature [8] as resulting from the singularity of the involved systems.

We note that the spectrum of the infinite Kronig-Penney periodic potential is absolutely continuous [11]. In such infinite periodic system one can not define, in contrast to bounded systems, any total length L or any ratio c of its total interval to total width. That is, the gaps in their energy spectrum, that do not depend on any such undefined L and c , can not be preserved or disappear, as in the bounded potential, merely by taking some limit or other values of these L and c . Thus, their spectrum is, as remarked, generally absolutely continuous [11]. There are, of course, the exceptional infinite periodic systems [7, 8, 9] mentioned in Section 5 which are characterized by nonvanishing gaps but for other reasons not related at all to any L and c . The bounded multibarrier potential discussed here allows one not only to define its total length L and the related ratio of its total interval to total width but also to express the location of each barrier [4, 5] and consequently the allowed energies in terms

of L and c . Thus, there may be found, as actually shown in Sections 3-4, specific values of L and c for which the gaps in the energy spectrum do not disappear even for large values of E or (and) large κ . Moreover, for large (and intermediate) L and small c the energy E as function of κ of the bounded multibarrier potential have been shown to have the form of periodic half squares which are jumpy and discontinuous at their vertical sides (see Figures 1-2 and 4-5). These discontinuities in the energy become small and insignificant only when L decreases as may be seen in Figure 3 for the $E > V$ case and in Figure 6 for the $E < V$ one. When L becomes very small the gaps in the energy spectrum becomes wider and periodic as seen from Figure 7.

In summary, we see that the bounded one-dimensional multibarrier potential demonstrates through the discontinuities of E , the nonvanishing gaps in its energy spectrum, its almost zero-range potential and its complete transmission that it is a singular system.

REFERENCES

References

- [1] “Quantum mechanics” 2nd edition by E. Merzbacher, John Wiley and sons, (1961);
- [2] “Quantum mechanics” by C. C. Tannoudji, B. Diu, And F. Laloe, John Wiley and Sons (1977).
- [3] “Introduction to solid state physics”, third edition, C. Kittel, John Wiley & Sons, New York, (1966).
- [4] D. Bar and L. P. Horwitz, Eur. Phys. J. B, **25**, 505-518, (2002); Phys. Lett A, **296**, 265-271, (2002).
- [5] D. Bar and L. P. Horwitz, J. Phys. B, **35**, 4915-4931, (2002).
- [6] A. Grossmann, R. Hoegh-Krohn and M. Mebkhout, J. Math. Phys, **21**, 2376-2385, (1980); “Solvable models in quantum mechanics”, by S. Albeverio, F. Gesztesy, R. Hoegh-Krohn and H. Holden, Springer, Heidelberg, (1988).
- [7] D. B. Pearson, Commun. Math. Phys, **60**, 13-36 (1978).
- [8] J. E. Avron, P. Exner and Y. Last, Phys. Rev. Lett, **72**, 896-899, (1994).
- [9] “Zero-range potentials and their applications in atomic physics”, by Yu. N. Demkov and V. N. Ostrovskii, Plenum Press, New York (1988).
- [10] S. Jitomirskaya and Y. Last, Phys. Rev. Lett, **76**, 1765-1769, (1996).
- [11] “Spectral theory of random Schrodinger operators”, by R. Carmona and J. Lacroix, Birkhouser, Boston (1990).

- [12] K. W. Yu, *Computers in Physics*, **4**, 176-178, (1990).
- [13] “The transition to chaos in conservative classical systems: Quantum manifestations”, L. E. Reichel, Springer, Berlin, 1992; E. Haller, H. Koppel and L. S. Cederbaum, *Chem. Phys. Lett*, **101**, 215-220, (1983); T. A. Brody, J. Flores, J. B. French, P. A. Mello, A. Pandey and S. S. M. Wong, *Rev. Mod. Phys*, **53**, 385, (1981).
- [14] “Methods of modern mathematical physics: Scattering theory” by M. Reed and B. Simon, Academic Press, (1979).
- [15] “Applied mathematics for engineers and physicists”, by L. A. Pipes, 2-nd edition, McGraw-Hill Book Company, New York, (1958).